On the Optimization of Superplastic Blow-Forming Processes

X.D. Ding, H.M. Zbib, C.H. Hamilton, and A.E. Bayoumi

The superplastic blow-forming process of thin sheets is analyzed, and an optimal stable deformation path that reduces production time is obtained. The analysis is based on an analytical model for the superplastic forming (SPF) of a long rectangular box made of Ti-6Al-4V alloy at 900 °C, use of a microstructure-based constitutive equation for the strain rate and grain growth, a stability criterion, and a variable strain rate control. It is shown that by imposing a variable strain rate control scheme derived from the stability analysis, an optimal forming time can be developed while maintaining a stable deformation path. Some other control schemes also show effectiveness in either reducing the localized thinning in the formed sheet or reducing the required forming time. Effects of friction and initial grain sizes on the forming pressure profile and the thickness distribution of the formed sheet are also investigated.

Keywords
superplastic forming, material stability, localized necking

1. Introduction

SUPERPLASTIC forming has become a widely used manufacturing process in the aircraft industry as well as in other applications where conventional processes have proved to be inadequate when production of complicated shapes is required. See Pellerin (Ref 1) and Stephen (Ref 2). In addition, this process offers a solution to the problem of noise pollution of the drop hammer forming process. SPF appears to be one of the processes to be used for off-loading parts usually formed with the drop hammer. As the SPF applications increase, there is increasing interest in numerical models that have the capability of predicting the forming characteristics, such as localized thinning and rupture, and that can establish forming parameters, such as gas pressure application to control strain rate; eventually the forming processes are optimized. For example, recent results suggest that a properly designed strain rate profile, which must be translated into a gas pressure profile for part forming, can be designed to substantially reduce the forming time from that of the current state-of-art technology. See, for example, Ash and Hamilton (Ref 3), Ren et al. (Ref 4), and Johnson et al. (Ref 5). These predictive tools however, require appropriate constitutive relations, flow rules, and a realistic quantitative description of the friction at the die/workpiece interface.

Because the SPF is a relatively slow process and an increase in productivity is required, it is often important to form as rapidly as possible while maintaining the required quality of the formed parts, such as eliminating localized thinning and rupture. In practical forming processes, many factors must be considered that affect the quality of the formed parts, such as material flow properties, process parameters, geometry, and friction effects. See Hamilton (Ref 6) and Ghosh and Hamilton (Ref 7). Here, we consider the material flow properties and their association with the process parameters, such as the control pressure cycle for blow forming, and friction.

The main objective of the present work is to develop an optimal pressure profile for the blow-forming process based on realistic constitutive equations, a rigorous stability analysis, and numerical simulations. Namely, we incorporate a microstructure-based constitutive equation into a simulation model for the analysis of superplastic forming of a sheet metal into a rectangular box. The constitutive equation for the flow stress, which includes the effect of grain growth, was developed by Hamilton et al. (Ref 8) for the Ti-6Al-4V alloy. Furthermore, we develop a number of pressure profiles by considering a variety of strain rate gradient controls. The strain rate control is based on a stability analysis developed for uniaxial extensions by Johnson et al. (Ref 5), who employed the necking criterion of Hart (Ref 9) to obtain an optimal variable strain rate path. See also Nichols (Ref 10). Thus, the pressure increment during the forming process is determined by the variation of the strain rate in the sheet from the target value set by the optimal path. This leads to a simple linear control relating the pressure to the percent deviation in strain rate. We also examine the case where the strain rate gradient in the sheet is also controlled, effectively controlling the localized thinning.

Since the strain rate field is nonuniform in the sheet, the strain rate control is employed over two different regions of the sheet, i.e. the free forming region and the die entry radius region. Namely, we develop several control schemes to generate the pressure profile and compare the results for forming time and thickness distributions. Five control schemes are considered: (1) constant strain rate control in the free forming region; (2) constant strain rate control in the die entry radius region; (3) variable strain rate control in the free forming region; (4) maximum variable strain rate control; and (5) maximum strain rate gradient control. It is shown that by using the schemes of the variable strain rate control in the free forming region and constant strain rate control in the die entry radius region, the forming time can be reduced without increasing the degree of thinning. However, when using the strain rate gradient control scheme, the excessive localized thinning in the formed sheet can be reduced, but a longer forming time is required. Finally,

X.D. Ding, H.M. Zbib, C.H. Hamilton, and **A.E. Bayoumi,** Department of Mechanical and Materials Engineering, Washington State University, Pullman, WA 99164-2920, USA.

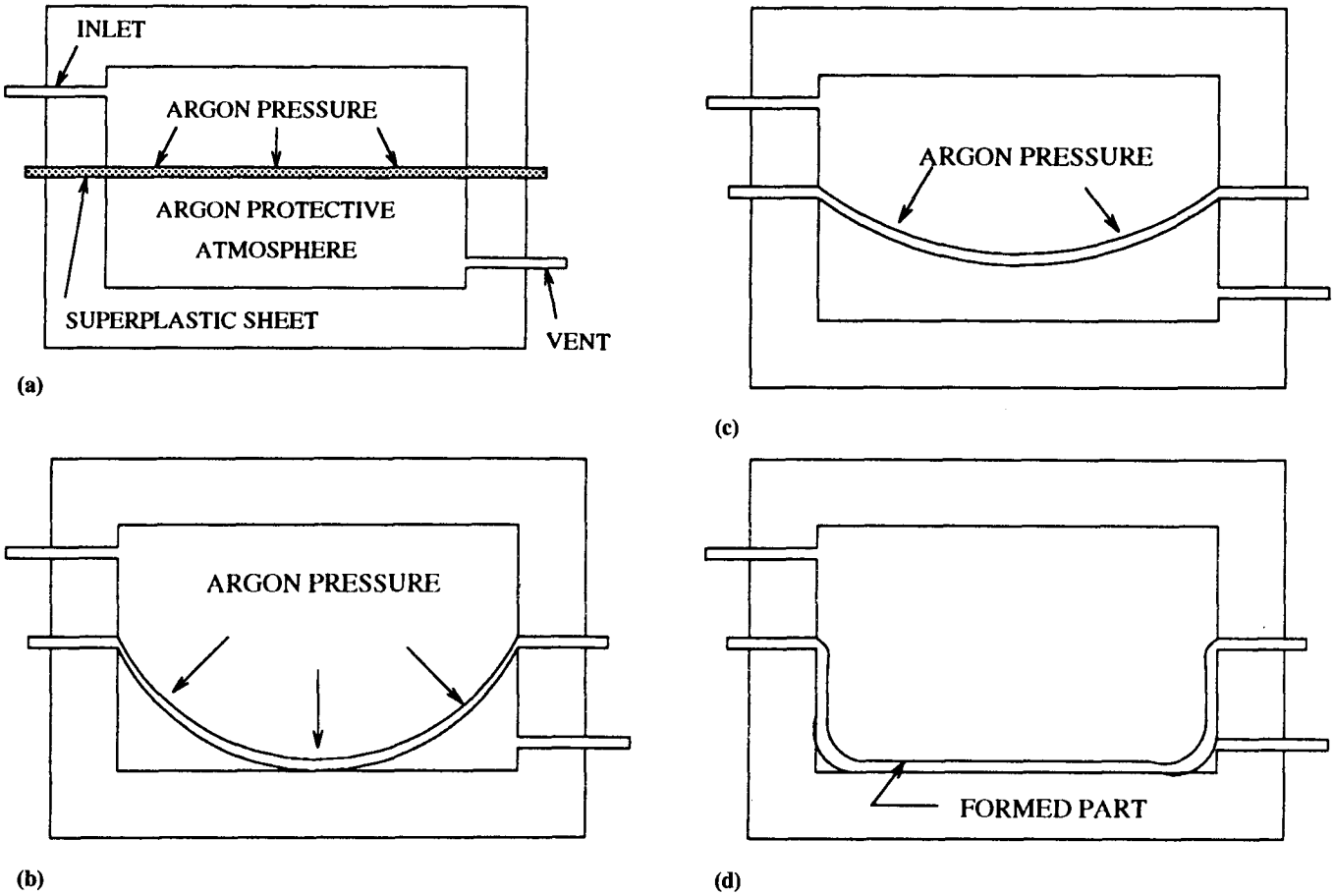

Fig. 1 Illustration of the blow-forming process for superplastic forming (Ref 11)

the effect of friction (lubrication) and initial grain size (hardening) on the forming time and thinning is investigated by considering different friction coefficients and initial grain sizes. It is shown that increasing the initial grain size causes sever localization, supporting the belief that a finer grain size is more desirable for achieving a better formability. Similarly, it is shown that as the friction coefficient increases, the forming time increases with an increase in forming pressure and in the degree of nonuniformity of thickness distribution.

2. Analytical Model

In this work, we investigate the superplastic forming of a long rectangular box section as a case study to establish and examine various deformation paths based on the controls discussed in the previous section. The problem of a long rectangular box was examined by Ghosh and Hamilton (Ref 11), who developed a numerical model to simulate the forming process. (The problem also was treated by other researchers. See for example Ref 12 to 17.) In this work, we employ the same model but modify it to include a microstructure-based constitutive equation for the flow stress along with an evolution equation for the grain size. Furthermore, we incorporate the various control schemes in the analysis.

2.1 *Simulation Model*

The blow-forming process of a long rectangular box section examined in this work is illustrated in Fig. 1. Since the flow stress is relatively low, superplastic sheets are blow formed by one-sided gas pressure in a die as shown in the figure. In the forming of Ti-6Al-4V at 900 °C, an inert atmosphere is also required, and argon gas is generally used for both pressurization and maintenance of a protective atmosphere.

The simulation model developed by Ghosh and Hamilton (Ref 11) is used in this work but with a different constitutive equation and pressure control as discussed in the next sections. Thus, the details of the numerical analysis are similar to those established in Ref 11. Here we give only a brief description of the model. The long rectangular box or channel section considered is a shape common to many actual parts and permits a nearly plane strain state to be established in most of the part. Therefore, along the midsection normal to the length, the stress state is assumed to be plane strain, thus requiring a one-dimensional membrane analysis. Figure 2 is a cross-section view of the forming die and superplastic alloy sheet. Due to symmetry, only half of the box is analyzed. Since the excessive localized

Table 1 Die and sheet data used in the simulation

Symbol	Definition	Value
h_0	Initial sheet thickness	0.066 in. (1.68 mm)
W	Half of die width	2 in. (50.8 mm)
D	Die depth	2 in. (50.8 mm)
r	Die entry radius	0.08 in. (2.03 mm)
A	Flange length	0.5 in. (12.7 mm)
R_{min}	Minimum edge radius	0.08 in. (2.03 mm)
μ	Friction coefficient	0.0, 0.1, 0.2, 0.3, 1

Table 2 Material parameters used in the simulation

Symbol	Definition	Value
d_0	Initial grain size	4 to 10 μm
B	Time constant	0.1647 μs
q	Grain growth exponent	4.9
K_4	Dynamic grain growth factor	1.72×10^4
σ_0	Threshold stress	25.0 N/cm^2
m	Strain rate sensitivity parameter	0.7
N	Stress exponent	4.3
$\bar{A}$	Region 2 factor	3.06×10^{-18}
$\bar{D}$	Region 3 factor	3.5×10^{-20}
P	Grain size exponent	3.0
τ	Vacancy relation time	3148 s

thinning occurs over the die entry radius region, the model considers the regions of the die entry radius, r, and flange length, A, in detail. This is accomplished by considering a fine mesh in these regions as shown in Fig. 2(a). Frictional effects over the die entry radius, flange, bottom, and side walls are also considered and permit the examination of cases of low sliding friction as well as high sticking friction. Finally, the model considers the excessive localized thinning occurring over the die entry radius and incorporates realistic die and sheet frictional effect; i.e., it allows sliding to occur. Pressurization cycles are developed by controlling the strain rate or strain rate gradient according to different control schemes. Table 1 lists the die and sheet data used in the simulation. See Ghosh and Hamilton (Ref 11) for more details of the numerical model.

2.2 *Constitutive Equations*

The constitutive relation for superplastic materials utilized in this study is based on the assumption that independent deformation mechanisms may act within the superplastic strain rate region 2 and the power-law creep region 3 as explained by Johnson et al. (Ref 5). Their analysis leads to the following relation for the total plastic strain rate under isothermal conditions.

$$\dot{\varepsilon} = \frac{\bar{A}(\sigma - \sigma_0)^{\frac{1}{m}}}{d^p} + \bar{D}\sigma^N \qquad \text{(Eq 1)}$$

where $\bar{A}$, and $\bar{D}$ are material parameters, d is the average grain size, p is the grain size exponent, σ_0 represents an internal stress or a threshold stress, m is the strain rate sensitivity, and N is the power-law exponent. Values for $\bar{A}$, σ_0, $\bar{D}$, m, N, and p

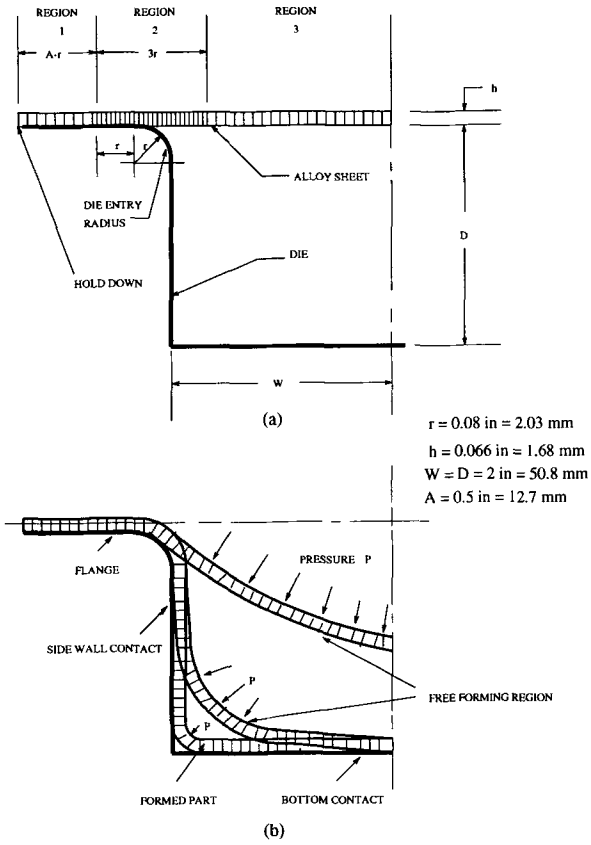

Fig. 2 Sheet and die model

were measured experimentally for Ti-6Al-4V alloy and are given in Ref 5.

The stress and strain rate behavior of Ti-6Al-4V alloy is well known to be strongly dependent on grain size. It was shown that grain coarsening occurs during deformation and causes flow hardening as well as changes in the m value. The total grain growth kinetics are assumed to result from a static grain growth rate, $\dot{d}^{\sigma}$, and a deformation-enhanced grain growth, $\dot{d}^{\delta}$, and are expressed as (Ref 5):

$$\dot{d} = \dot{d}^{\delta} + \dot{d}^{\sigma} = \frac{B}{d^q} + \frac{K_4(1 - e^{-\frac{t}{\tau}})}{d^{q-1}}\dot{\varepsilon} \qquad \text{(Eq 2)}$$

where q is a constant, B is a function of temperature, K_4 and τ are constants whose physical meanings are discussed in Ref 5. Figure 3 is the stress and strain rate relation at 900 °C for the Ti-6Al-4V alloy calculated from Eq 1 and 2. Table 2 provides the material parameters used in the analysis. They were determined experimentally in Ref 5.

2.3 *Stability Criterion: Optimal Strain Rate Path*

The stretching of superplastic sheets is limited by the onset of localized necking resulting from unstable deformations. The onset of instability and the strain at which it occurs determines

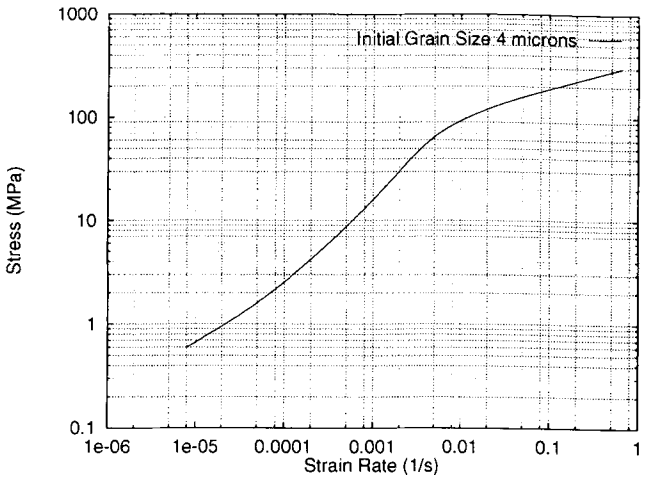

Fig. 3 Stress and strain rate relation for Ti-6Al-4V at 900 °C

the stretchability of the sheet. Thus, for the case of a uniaxial stretching, the onset of instability in the form of necking can be determined following the analysis of Hart (Ref 9). This analysis is based on the assumption of an initially uniform plastic deformation that becomes unstable when $\delta \ln \dot{A}/\delta \ln A \leq 0$, where A is the instantaneous cross-section of the sheet. Using the constitutive equation:

$$\sigma = \sigma(\varepsilon,\dot{\varepsilon}) \qquad \text{(Eq 3)}$$

where σ is the flow stress. Hart (Ref 9) derived the criterion:

$$\gamma + m = 1$$

$$\gamma = \frac{\partial \sigma}{\partial \varepsilon}\frac{1}{\sigma}\Big|_{\dot{\varepsilon}}$$

$$m = \frac{\partial \sigma}{\partial \dot{\varepsilon}}\frac{\dot{\varepsilon}}{\sigma}\Big|_{\varepsilon} \qquad \text{(Eq 4)}$$

for the onset of instability, with γ being the strain hardening exponent and m the strain rate sensitivity exponent.

In our case, the constitutive equation is given by Eq 1 with a dependence on the grain size for which evolution is given by Eq 2. These two equations can be written formally as:

$$\begin{aligned} \dot{\varepsilon} &= f(\sigma,d) \\ \dot{d} &= g(\dot{\varepsilon},d) \end{aligned} \qquad \text{(Eq 5)}$$

Then following the procedure developed by Hart for the onset of necking instability, we obtain the corresponding criterion:

$$\gamma' + m' = 1$$

$$\gamma' = \frac{\dot{d}}{\dot{\varepsilon}^2}\frac{\partial \dot{\varepsilon}}{\partial d}\Big|_{\sigma}$$

$$m' = \frac{\sigma}{\dot{\varepsilon}}\frac{\partial \dot{\varepsilon}}{\partial \sigma}\Big|_{d} \qquad \text{(Eq 6)}$$

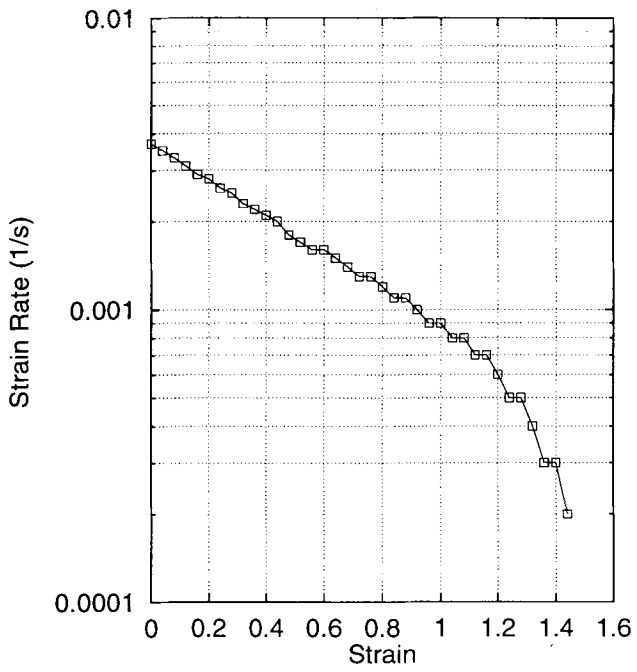

Fig. 4 Optimal variable strain rate path

where γ' is the grain hardening exponent and m' is the inverse of the strain rate sensitivity ($m' = 1/m$). Thus, at a given strain rate, Eq 6 gives the value of d, which corresponds to some specific time t and strain ε, through the integration of Eq 1 and 2. The result of the analysis is given in Fig. 4, which gives the critical strain for a given strain rate for the Ti-6Al-4V alloy. Thus, it provides a critical strain rate path that can be imposed without causing an unstable deformation. This would also be an optimal path in the sense of a stable path that would yield the least forming time up to a specified strain.

Formally, the condition for the onset of instability (Eq 6) can be written in the form:

$$G(\dot{\varepsilon}, d) = \gamma' + m' - 1 = 0 \qquad \text{(Eq 7)}$$

or

$$\overline{G}(\dot{\varepsilon},\varepsilon) = 0 \qquad \text{(Eq 8)}$$

because, for a given $\dot{\varepsilon}$, d and ε can be evaluated from Eq 1 and 2. Thus, the solution of Eq 8 gives the optimal strain rate path, $\dot{\varepsilon}^*$:

$$\dot{\varepsilon}^* = H(\varepsilon) \qquad \text{(Eq 9)}$$

For the Ti-6Al-4V alloy under consideration, this path is determined numerically using Eq 1, 2, and 6, yielding the graph shown in Fig. 4. It turns out that this curve can be fitted to the polynomial relation:

$$\dot{\varepsilon}^* = a - b\varepsilon + c\varepsilon^2 - d\varepsilon^3 \qquad \text{(Eq 10)}$$

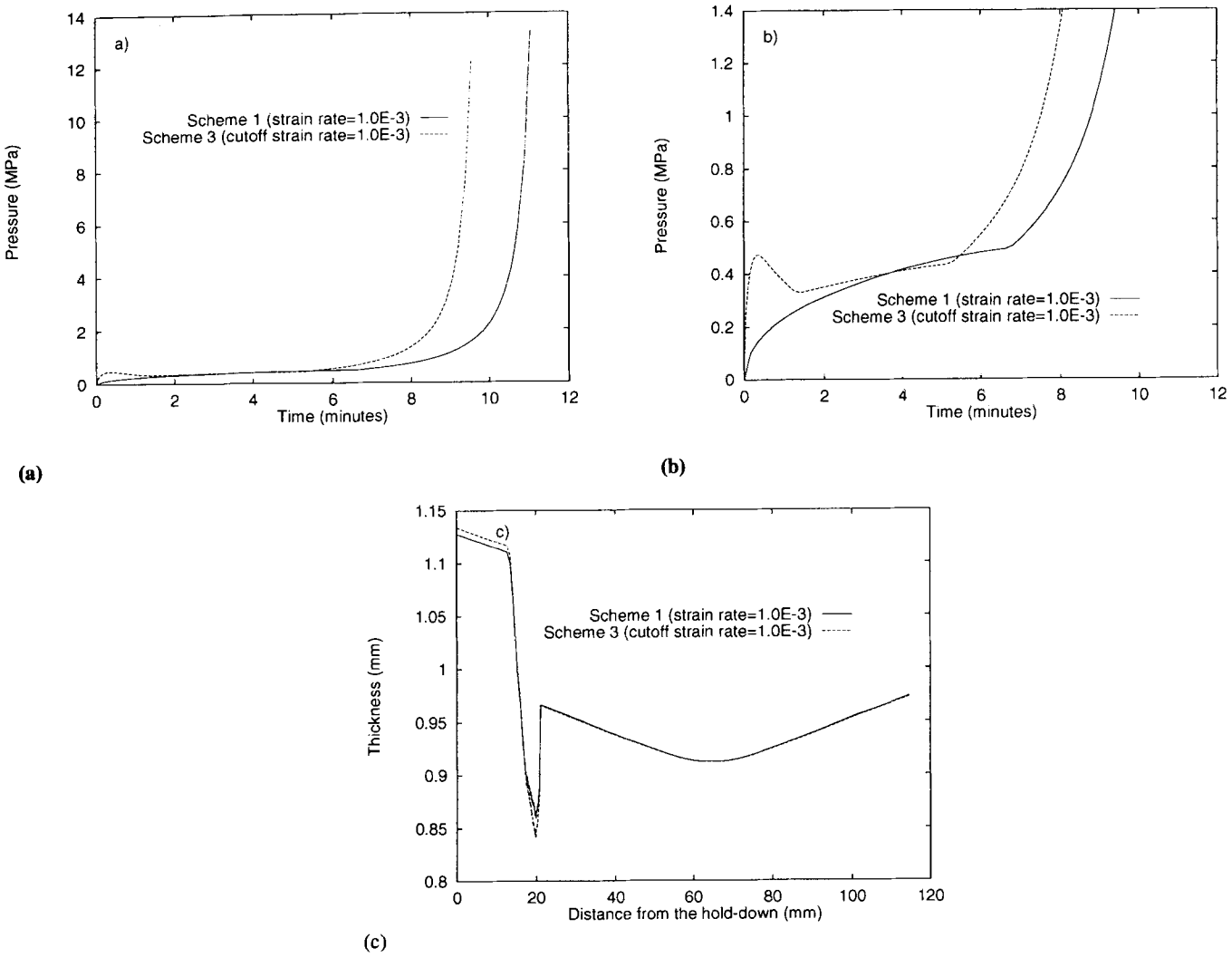

Fig. 5 Comparison of constant $\dot{\varepsilon}$ control in the free forming region (scheme 1) and variable $\dot{\varepsilon}$ control in the free forming region (scheme 3).

where

$a = 3.7026 \times 10^{-3}\ s^{-1}$
$b = 5.4345 \times 10^{-3}\ s^{-1}$
$c = 3.8375 \times 10^{-3}\ s^{-1}$
$d = 1.2243 \times 10^{-3}\ s^{-1}$

3. Control Schemes

A constant strain rate control in the free forming region (or unsupported region) is an established method to generate the pressure cycle for the blow-forming process. In this method, the pressure is varied in such a way that the strain rate within the free forming region remains constant (Ref 11). The only restriction is that the value of this constant should lie within the superplastic strain rate region 2. However, excessive localized thinning in some parts of the formed sheet may occur due to the effect of stress gradients. This gradient is mainly caused by the different configurations of the die geometry, such as die entry radius in this case. Moreover, since the superplastic forming process is a relatively slow process due to a required small strain rate, some forming processes are very time consuming depending on the superplastic alloys used. In order to address these problems, several control schemes are explored to find the optimal pressurization cycles for the blow-forming processes, utilizing the optimal strain rate path given by Eq 10.

The main idea in controlling the deformation path is to vary the pressure in such a way that the strain rate $\dot{\varepsilon}$ in a certain specified region or node of the sheet reaches a desired value (target strain rate $\dot{\varepsilon}_T$). Thus, during the numerical calculation, at each increment, the initial pressure value is determined according to the mechanical model of Ghosh and Hamilton (Ref 11). Then, an iteration procedure is performed to adjust the pressure value to achieve the target strain rate in a desired region. This is accomplished by first evaluating the difference:

$$\Delta\dot{\varepsilon} = \dot{\varepsilon} - \dot{\varepsilon}_T \qquad \text{(Eq 11)}$$

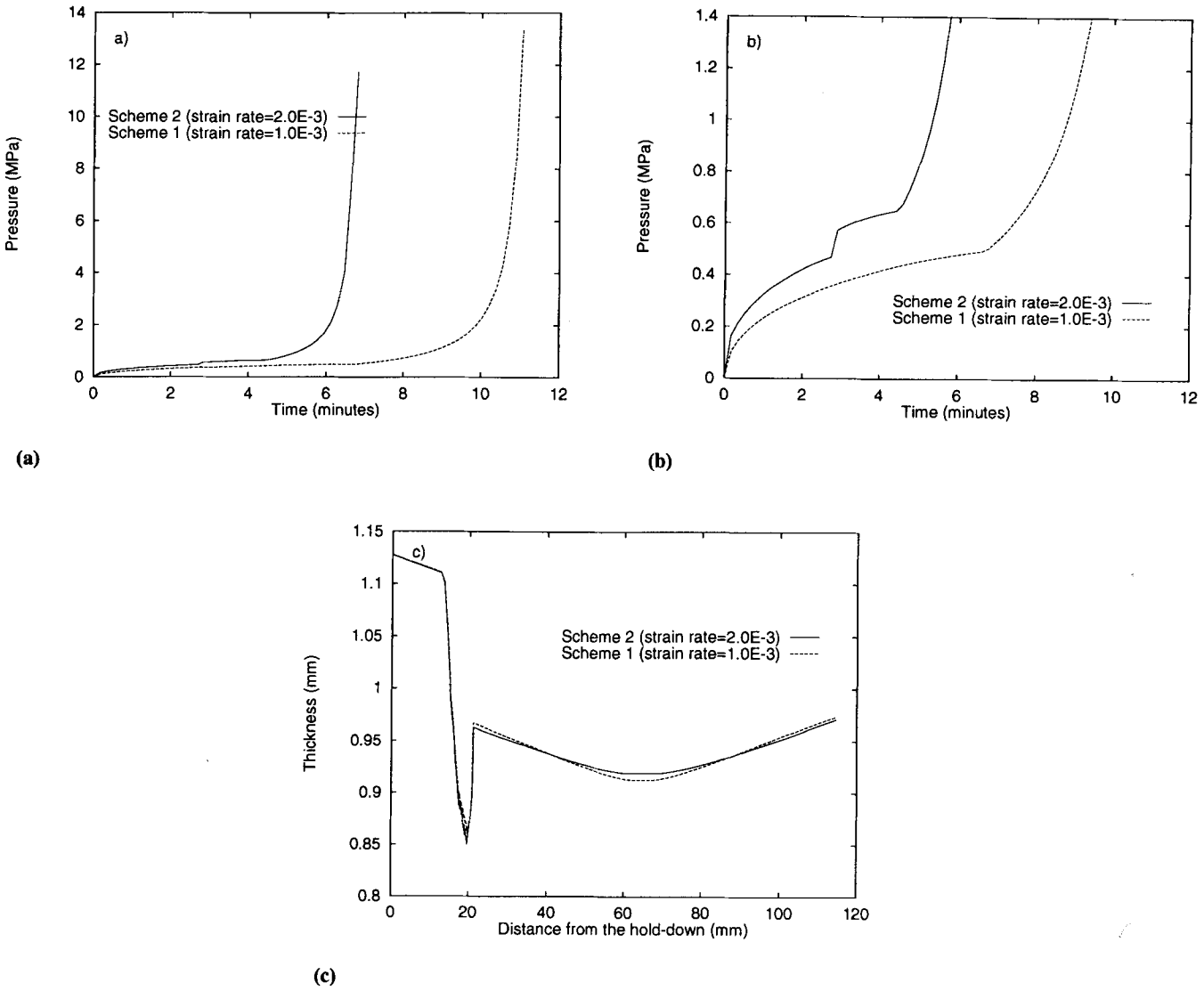

Fig. 6 Comparison on constant $\dot{\varepsilon}$ control in the free forming region (scheme 1) and constant $\dot{\varepsilon}$ control in die entry radius region (scheme 2). (a) Pressure profile. (b) Blow-up of figure (a). (c) Thickness distribution profile

Then, if this difference is negative, the pressure should be increased to produce an increase in the strain rate. If $\Delta\dot{\varepsilon} \leq 0$, a simple linear proportional controller of the form:

$$P^{i+1} = P^i(1 + e)$$

$$e = \frac{|\Delta\dot{\varepsilon}|}{\dot{\varepsilon}_T} \qquad \text{(Eq 12)}$$

where i is the iteration index and e is the error-target ratio, seems to yield fast convergence. (In a more general treatment, one would control the pressure rate $\dot{P}$ instead of the pressure so that $\dot{P}^{i+1} = \dot{P}^i(1 + e)$. In such a case, one needs only to specify an initial pressure rate value. This will be implemented in a general finite element program.) However, if the difference is positive, the pressure should be decreased. For this case, if $\Delta\dot{\varepsilon} \leq 0$, a controller of the form:

$$P^{i+1} = \frac{P^i}{1 + e} \qquad \text{(Eq 13)}$$

is suggested and seems to produce fast convergence. For this case, one could also use the proportional controller $P^{i+1} = P^i(1 - \Delta\dot{\varepsilon}/\dot{\varepsilon}_T)$. However, this may result in an anomalous result when $\Delta\dot{\varepsilon}/\dot{\varepsilon}_T \leq 1$, requiring a zero or negative pressure. This situation, if it occurs, can be handled easily using the controller given by Eq 13, suggesting a decrease in the pressure value since the denominator is always larger than or equal to one.

The following control schemes are investigated in this work.

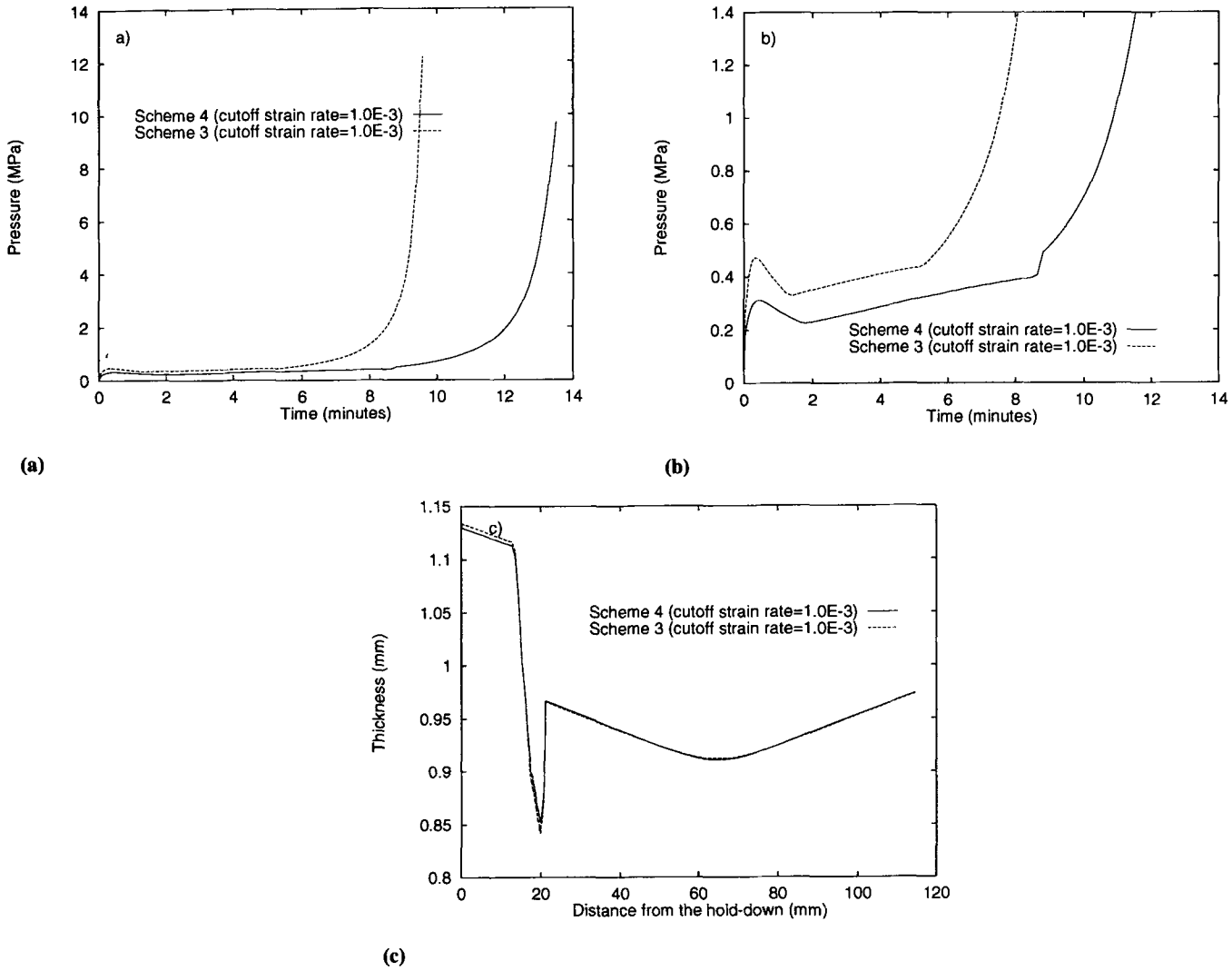

Fig. 7 Comparison of variable $\dot{\varepsilon}$ control in the free forming region (scheme 3) and variable $\dot{\varepsilon}$ control in the whole forming region (scheme 4). (a) Pressure profile. (b) Blow-up of figure (a). (c) Thickness distribution profile

3.1 *Scheme 1: Constant Strain Rate Control in the Free Forming Region*

The pressure cycle in this case is developed by maintaining a constant strain rate in the unsupported part of the forming sheet. Since this is an established method, its corresponding pressure and thickness distribution profiles of the formed sheet are used as bases for comparison with other control schemes.

3.2 *Scheme 2: Constant Strain Rate Control in the Die Entry Radius Region*

In this scheme, a constant strain rate is imposed on a certain node in the die entry radius region at the initial stage of forming. The chosen node corresponds to the maximum thinning point in the formed sheet where the strain rate is maximum at the early stage of deformation. The strain rate can be the maximum strain rate corresponding to the stable deformation without localized necking and rupture. This strain rate depends on material properties for a given die geometry, especially the initial grain size. After the forming sheet is in full contact with the die entry radius region, the control is switched back to controlling the free forming region with a constant strain rate.

3.3 *Scheme 3: Variable Strain Rate Control in the Free Forming Region*

Here the control is based on the stability analysis developed in section 2.3. The pressurization cycle is generated by controlling the strain rate in the unsupported part of the forming sheet using Eq 10. Since the strain rate decreases with strain, a constant strain rate is maintained when the strain rate reaches a certain low level. This strain rate is called the cutoff strain rate.

3.4 *Scheme 4: Maximum Variable Strain Rate Control*

Based on the numerical analysis, it is observed that during the initial stage of forming, the maximum strain rate occurs in

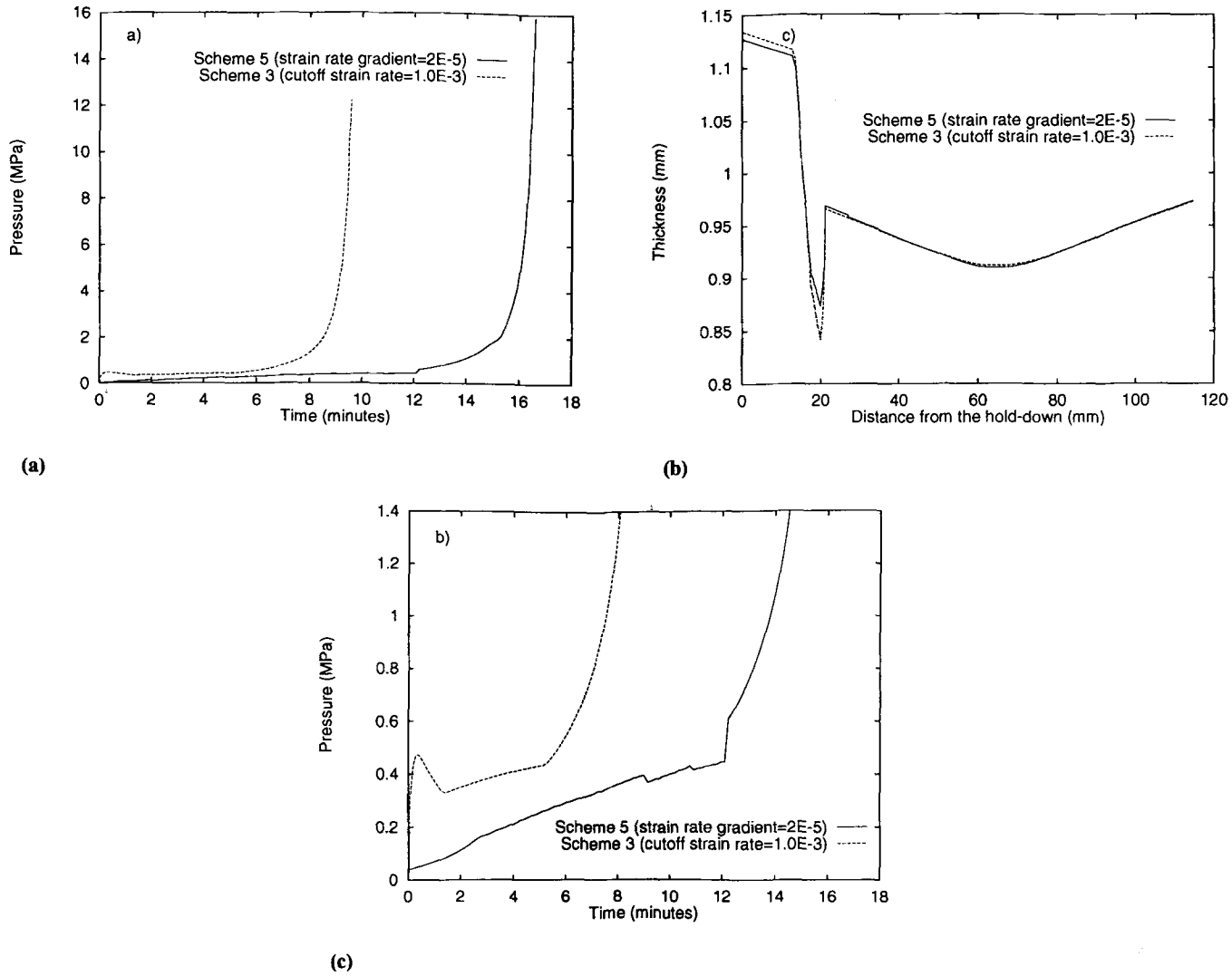

Fig. 8 Comparison of variable $\dot{\varepsilon}$ control in the free forming region (scheme 3) and maximum $\dot{\varepsilon}$ gradient control in die entry radius region (scheme 5). (a) Pressure profile. (b) Blow-up of figure (a). (c) Thickness distribution profile

the die entry radius region due to the effect of stress concentration. Thus, when we impose a constant or a variable strain rate in the free forming region, the strain rate in the die entry radius region is much higher than that in the free forming region. However, in the final stage of forming when the sheet is in complete contact with the die entry radius region, the maximum strain rate occurs in the free forming region. Thus, we develop a control scheme that is based on controlling the strain rate in the region with the maximum instantaneous strain rate. In this scheme, at each time increment, we check the strain rate at all the nodes of the forming sheet and calculate the forming pressure for the next increment according to the node with maximum strain rate using the variable strain rate path. Thus, the strain rate at all nodes is less than or equal to the target strain rate throughout the deformation history.

3.5 *Scheme 5: Maximum Strain Rate Gradient Control*

The numerical analysis shows that nonuniform superplastic deformation is caused by strain rate gradient in the forming sheet due to stress gradient, friction, and some other effects. For the blow-forming process under consideration, excessive thinning occurs in the die entry radius region of the formed sheet as can be deduced from Fig. 5 to 8. Moreover, under constant die geometry and friction conditions, the rate of forming is the main parameter affecting the rate of localized thinning. Thus, one could reduce the degree of thinning by controlling the strain rate gradient and the rate of loading. This is done here by first evaluating the strain rate gradient g in each element at each time increment, i.e.:

$$g \equiv \frac{\dot{\varepsilon}_{i+1} - \dot{\varepsilon}_i}{\Delta x} \qquad \text{(Eq 14)}$$

where i is the node number and Δx is the distance between two adjacent nodes. Then, a maximum allowable strain rate gradient g_T is imposed. If the strain rate gradient g in any element is larger than the allowable value g_T (if $g > g_T$), the pressure is reduced according to the controller:

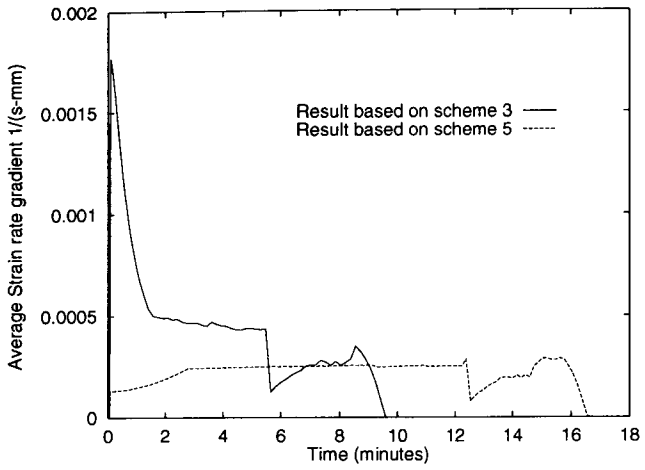

Fig. 9 Average strain rate gradient distribution based on schemes 3 and 5

$$P^{i+1} = \frac{P^i}{1+e}$$

$$e = \frac{g - g_T}{g_T} \qquad \text{(Eq 15)}$$

However, if $g \leq g_T$, no correction due to strain rate gradient is taken, and the pressure is controlled by either scheme 1 or scheme 3.

In the present analysis, since the die entry radius region has the greatest contribution to the strain rate gradient variation in the forming sheet, the average strain rate gradient in this region is calculated in the practical implementation so as to reduce computation time.

4. Discussion of Results

A number of simulation tests were conducted using the model and control schemes developed. To compare the effectiveness of the control schemes, comparisons of the results of the different schemes are discussed by analyzing the pressure and thickness distribution profiles. Effects of the initial grain size and friction on the forming processes are also presented.

4.1 *Comparison of Control Schemes*

In order to compare the pressure and thickness distribution profiles of different control schemes, the same set of geometrical, material, and process parameters is used for the simulations. Comparisons among all cases are discussed below.

4.1.1 Comparison between Schemes 1 and 3

Figure 5 shows the pressure and thickness distribution profiles of the twi\o schemes. Recall that scheme 1 is based on a constant strain rate control in the free forming region. (For the material under consideration, we use $\dot{\varepsilon} = 10^{-3}s^{-1}$, which lies in the superplastic region 2.) Scheme 3 is a variable strain rate control in the free forming region with a minimum cutoff strain rate of $\dot{\varepsilon} = 10^{-3}s^{-1}$. We see from Fig. 5(a) and (b) that the pre-

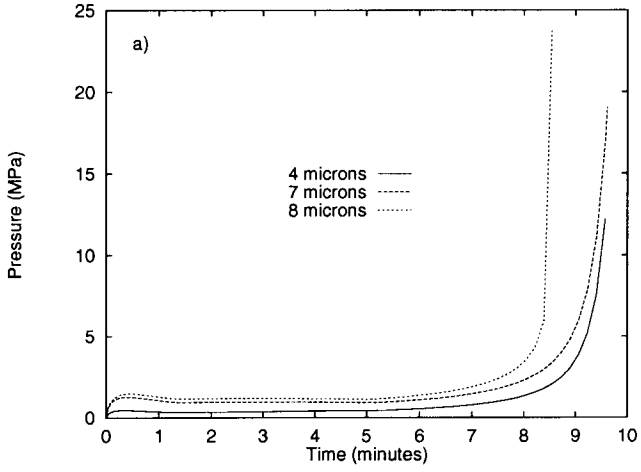

(a)

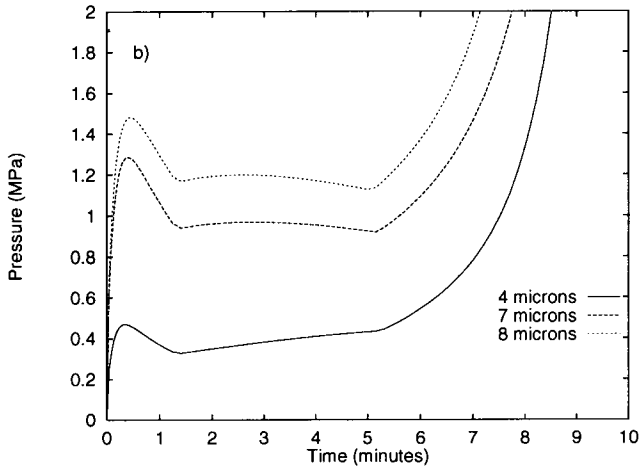

(b)

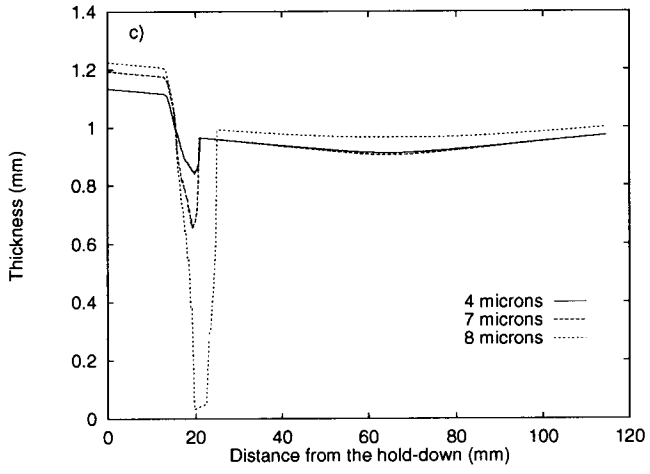

(c)

Fig. 10 Comparison of initial grain size effect (scheme 3). (a) Pressure profile. (b) Blow-up of figure (a). (c) Thickness distribution profile

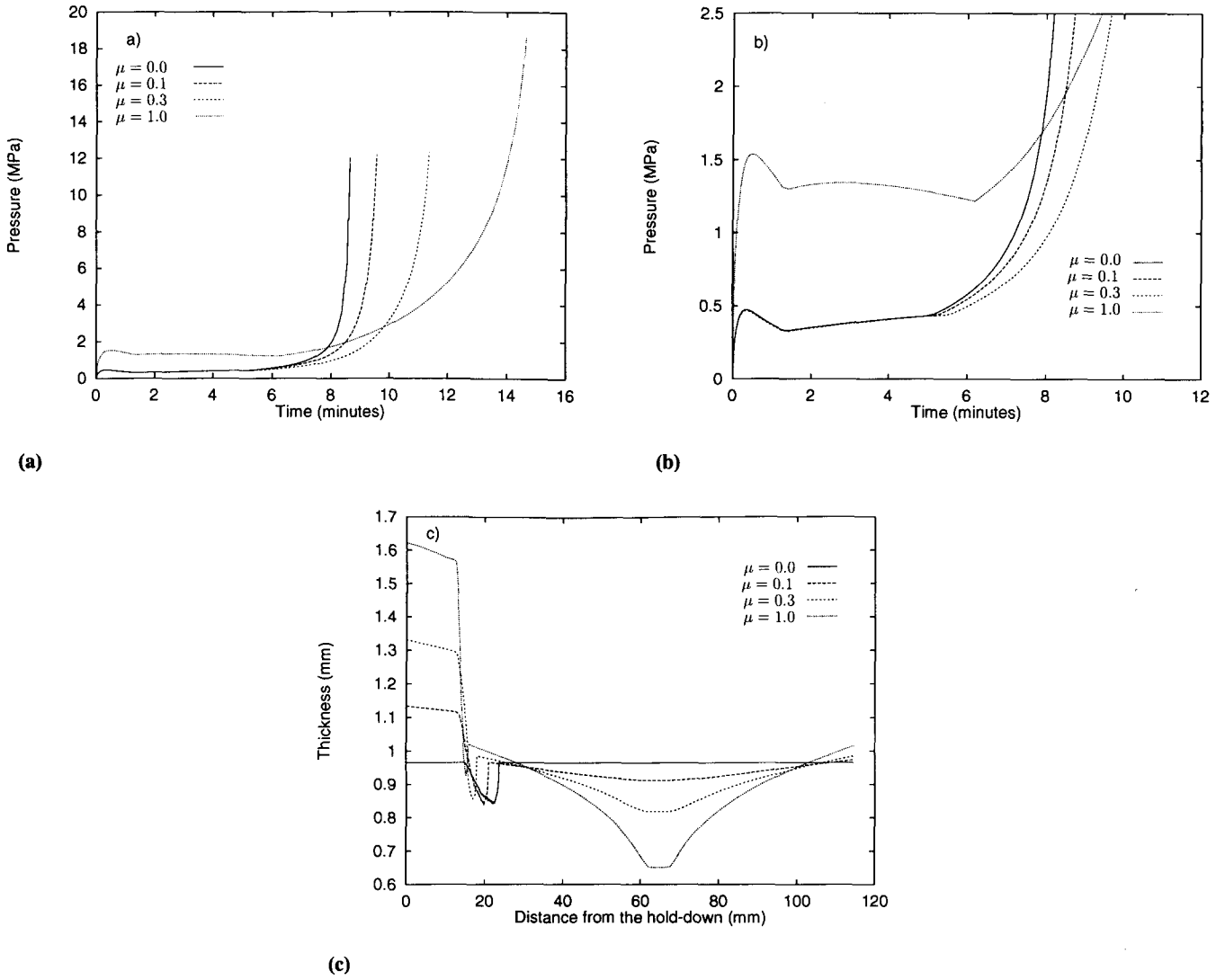

Fig. 11 Comparison of frictional effect (scheme 3). (a) Pressure profile. (b) Blow-up of figure (a). (c) Thickness distribution profile

dicted pressure increases with time for both cases. However, it can be deduced from the figures that the total forming time (where the pressure increases rapidly when the sheet is in full contact with the die) for scheme 3 is less than that of scheme 1. In fact, with scheme 3, we have a 13.4% saving in forming time. This, however, does not seem to influence the thickness distribution and localized thinning as shown in Fig. 5(c) where the difference at the localized point is only 2.1% between the two profiles. The result is reasonable since the forming strain rate in scheme 3 is larger than $10^{-3}s^{-1}$ at the initial stage of forming, and the grain growth effect is not large enough to cause more thinning as a result of increasing stress gradient.

4.1.2 Comparison between Schemes 1 and 2

For this case, again we use $\dot{\varepsilon} = 10^{-3}s^{-1}$ for scheme 1. For scheme 2, which is a constant strain rate control in the die entry radius region, we use $\dot{\varepsilon} = 2 \times 10^{-3}s^{-1}$ (in the superplastic region 2). The results are shown in Fig. 6(a) to (c). Figures 6(a) and (b) show that scheme 2 is much faster than scheme 1 with a 38.4% saving in forming time, and it is even faster than scheme 3. Furthermore, there is not much difference in the thickness distribution profiles between the two cases as shown in Fig. 6(c). However, the highest strain rate we can impose for scheme 2 depends upon the initial grain size. If the initial grain size is large, we cannot impose high strain rate because excessive thinning may occur or may even lead to rupture. This is discussed further in section 4.2.

4.1.3 Comparison between Schemes 3 and 4

Figure 7 shows the pressure and thickness distribution profiles of schemes 3 and 4 (variable strain rate control in the region with maximum instantaneous strain rate). As shown, scheme 4 needs more forming time than scheme 3 (41% more) and more time than scheme 1 (22% more). However, the thickness distribution profile remains similar to those of schemes 3 and 1. The result is as expected since we are actually imposing a lower strain rate in the die entry radius region than both schemes 3 and 2.

4.1.4 Comparison between Schemes 3 and 5

Figure 8 shows the pressure and thickness profiles of scheme 5 compared with those of scheme 3. For scheme 5, a strain rate gradient control is superimposed on scheme 3. Since the maximum strain rate gradient (g) occurs in the die entry radius region, we impose a ceiling value (g_T) on the average strain rate gradient value of the die entry radius region. A typical strain rate gradient distribution is shown in Fig. 9. Here we choose a strain rate gradient $g_T = 3.0 \times 10^{-4} s^{-1}$/mm as a ceiling value. Figure 9 shows that the strain rate gradient distribution based on scheme 5 is less than the ceiling value. The result shows that 4% less thinning is achieved, and the forming process is slowed down considerably with an increase of 73% in forming time compared to scheme 3. Further reduction in thinning can be achieved by decreasing the ceiling value g_T, but this would result in an increase in the forming time. Thus, there is a trade-off between forming time and localized thinning.

4.2 *Effect of Initial Grain Size*

Since a microstructure-based constitutive equation is utilized in the simulation, the grain size effect on the forming processes can be studied in detail with emphasis on initial grain size. Scheme 3 is employed to perform this simulation using the forming strain rate $\dot{\varepsilon} = 10^{-3} s^{-1}$. The results are shown in Fig. 10. Figures 10(a) and (b) show that as the initial grain size increases from 4 μm to 8 μm, the pressure value increases for the same forming time, but there is not much difference in the required final forming times. From the thickness distribution profiles, we see that the localized thinning near the die entry radius region becomes more severe as the initial grain size is increased. In fact, for the 8 μm initial grain size case, the excessive thinning near the die entry radius region is so severe that rupture may occur. The results show that the initial grain size has a severe effect on the forming processes. This can be explained by the grain growth hardening effect (see Eq 1). As the initial grain size increases, the grain growth hardening effect increases so that higher pressure is required to overcome this hardening. Since the largest strain occurs near the die entry radius region, the greatest grain growth also occurs in this region and, as a result, causes the most localized thinning.

4.3 *Effect of Friction*

Frictional effects on the forming pressure and thickness distribution profiles of the formed sheets are studied. Simulations are done using scheme 3 with the friction coefficient μ ranging from 0.0 (no friction), 0.1, 0.2, 0.3 to 1. The results are shown in Fig. 11. From the results, it can be deduced that as the friction coefficient increases, the thinning gradient along the die entry radius region and bottom and side wall of the die also increases. When there is no friction (μ = 0.0), the formed sheet is uniform in thickness distribution except near the die entry radius region because there is a stress gradient in this region due to curvature effects. When there is little sliding between the die and the sheet (i.e. μ = 1), the formed sheet has the most nonuniform thickness distribution, illustrating the significant effect of friction on the final thickness distribution of the product.

5. Conclusions

In summary, the constant strain rate control in the free forming region (scheme 1), as an established control method, has been used as an effective control scheme for blow-forming processes. However, for some die geometry and superplastic alloys, the forming time may be too long, or unsatisfactory thickness distribution of the formed sheet may occur. In practical applications, there may be two factors to consider for superplastic blow-forming processes. One is to reduce the forming time, which can lead to high productivity. The other is to increase the uniformity or required thickness distribution of the formed sheet, which may result in a higher quality part. In order to achieve this goal, exploring other control methods is a worthwhile work. In this research, we propose several control schemes. The numerical results show that it is possible to reduce the forming time or improve the thickness distribution of the formed sheet, but it is difficult to achieve both at the same time. From the simulation results and comparisons, we conclude the following.

- The variable strain rate control in the free forming region (scheme 3) is an efficient method for superplastic blow-forming processes in which the forming time is reduced significantly while maintaining a stable deformation. However, the variable strain rate path used in this analysis is based on a uniaxial state of stress that needs to be further extended to the biaxial state of stress.
- The constant strain rate control in the die entry radius region (scheme 2) gives a good result in forming time reduction. But the constant strain rate imposed is chosen arbitrarily within superplastic region 2. Therefore, experiments for the maximum strain rate value that can be imposed are needed before it is used in practical forming operations.
- The maximum strain rate gradient control (scheme 5) is very time consuming. However, if a reduction in the localized thinning is required, without regard to the forming time, it is nevertheless an effective control method.
- The other control scheme (4) is less effective in terms of the requirements mentioned above. They may be applicable in some forming operations, but experiments are needed to verify their applicability.
- The friction between the die and the forming sheet affects the forming process significantly. As the friction coefficient increases, the thickness distribution becomes more nonuniform, and more forming time is required.
- The initial grain size has a severe effect on the localized thinning of the forming sheet. As the initial grain size increases, severe localization occurs at the die entry radius region.

Acknowledgment

The support of the National Science Foundation under grant No. DDM-9114852 is gratefully acknowledged.

References

1. C.J. Pellerin, Air Force Perspective on SPF and SPF/DB Titanium Technology, *Superplastic Forming*, 1984, p 63-69

2. D. Stephen, Designing for Superplastic Alloys, *Superplasticity*, NATO Report AGARD-LS-168, Advisory Group for Aerospace Research and Development, NATO, Neuilly-Sur-Seine, France, 1989, p 7.1-7.37
3. B.A. Ash and C.H. Hamilton, Strain and Strain Rate Hardening Characteristics of a Superplastic Al-Li-Cu-Zr Alloy, *Scr. Metall.*, Vol 22, 1988, p 277-282
4. B. Ren, C.H. Hamilton, and B.A. Ash, An Approach to Rapid SPF of an Al-Li-Cu-Zr Alloy, *Fifth International Aluminum-Lithium Conference*, 1989
5. C.H. Johnson, C.H. Hamilton, H.M. Zbib, and S.K. Richter, Designing Optimized Deformation Paths for Superplastic Ti-6Al-4V, *Advances in Superplasticity and Superplastic Forming: I*, N. Chandra et al., Ed., The Minerals, Metals and Materials Society, 1993, p 3-15
6. C.H. Hamilton, Superplastic Sheet Forming, *NATO/AGARD Lecture Series No. 168, Superplasticity*, 1989, p 2.1-2.23
7. A.K. Ghosh and C.H. Hamilton, Influences of Material Parameters and Microstructure on Superplastic Forming, *Metall. Trans. A*, Vol 13, 1982, p 737-743
8. C.H. Hamilton, H.M. Zbib, C.H. Johnson, and S.K. Richter, Microstructural Coarsening and its Effect on Localization of Flow in Superplastic Deformation, *Superplasticity in Advanced Materials*, S. Hori, M. Tokizame, and N. Frushiro, Ed., The Japan Society of Research on Superplasticity, 1991, p 127-133
9. E.W. Hart, Theory of The Tensile Test, *Acta Metall.*, Vol 15, 1967, p 351-355
10. F.A. Nichols, Plastic Instabilities and Uniaxial Tensile Ductilities, *Acta Metall.*, Vol 28, 1980, p 663-673
11. A.K. Ghosh and C.H. Hamilton, Superplastic Forming of a Long Rectangular Box Section—Analysis and Experiment, *Proceedings of American Society for Metals on Process Modeling—Fundamentals and Applications to Metals*, 1978, p 303-331
12. F. Jovane, An Approximate Analysis of the Superplastic Forming of a Thin Circular Diaphragm Theory and Experiments, *Int. J. Mech. Sci.*, Vol 10, 1968, p 403-427
13. W. Johnson, T.Y.M. Al-Naib, and J.L. Duncan, Superplastic Forming Techniques and Strain Distributions in a Zinc-Aluminum Alloy, *J. Inst. Met.*, Vol 100, 1972, p 45-50
14. T.Y.M. Al-Naib and J.L. Duncan, Superplastic Metal Forming, "Int. J. Mech. Sci., Vol 12, 1970, p 463-477
15. D.L. Holt, An Analysis of the Bulging of a Superplastic Sheet by Lateral Pressure, *Int. J. Mech. Sci.*, Vol 12, 1970, p 491-497
16. G.C. Cornfield and R.H. Johnson, The Forming of Superplastic Sheet Metal, *Int. J. Mech. Sci.*, Vol 12, 1970, p 479-490
17. G.G.W. Clemas, S.T.S. Al-Hassani, and W. Johnson, The Bulging of a Superplastic Sheet From a Square Die, *Int. J. Mech. Sci.*, Vol 17, 1975, p 711-718